G.654.E optical fibers for high-data-rate terrestrial transmission systems with long reach

John D. Downie, Sergejs Makovejs, Jason Hurley, Michal Mlejnek, Hector De Pedro

John D. Downie, Sergejs Makovejs, Jason Hurley, Michal Mlejnek, Hector De Pedro, "G.654.E optical fibers for high-data-rate terrestrial transmission systems with long reach," Proc. SPIE 10561, Next-Generation Optical Communication: Components, Sub-Systems, and Systems VII, 105610N (29 January 2018); doi: 10.1117/12.2297683

SPIE.

Event: SPIE OPTO, 2018, San Francisco, California, United States

G.654.E optical fibers for high data rate terrestrial transmission systems with long reach

John D. Downie*[a], Sergejs Makovejs[b], Jason Hurley[a], Michal Mlejnek[a], Hector DePedro[c]
[a]Corning, Sullivan Park, SP-AR-02-1, Corning, NY 14831; [b]Corning Incorporated, Lakeside Business Village, St. David's Park, Ewloe, CH5 3XD, UK; [c]Corning Incorporated, Center for Fiber-Optic Testing, Corning, NY 14831
*downiejd@corning.com; phone 1 607 974-2713; fax 1 607 974-9268

ABSTRACT

Data traffic demands continue to increase worldwide, driving requirements for higher spectral efficiency systems and higher individual channel capacities. To enable terrestrial transmission systems to keep up with demand, the ITU recently adopted the G.654.E standard for optical fiber with larger effective area for terrestrial use. To keep macrobend loss performance the same as for conventional G.652 fiber, the cable cutoff wavelength specification for the new fiber class was increased to the lower edge of the C-band. We examine here several aspects of G.654.E fiber in terrestrial systems including modeled and experimentally measured transmission reach, the use of Raman amplification with pump wavelengths below cable cutoff, and the transmission of optical supervisory channels (OSC) at wavelengths below cable cutoff. We demonstrate significant transmission reach increases for 200 Gb/s PM-16QAM channels of at least 55% compared to standard single-mode fiber in a re-circulating loop experimental configuration. Addressing the practical questions of OSC and Raman pumps propagating below cable cutoff, we demonstrate experimentally and through extensive modeling that negligible impact is expected and observed in both cases.

Keywords: Optical fiber, OSNR, ultra-low loss, effective area, terrestrial, 16QAM.

1. INTRODUCTION

Large effective area (A_{eff}) ITU-T G.654 fibers have long been deployed in submarine networks, but are only now beginning to be adopted by the terrestrial transmission system industry. Until this point, ITU-T G.652 standard compliance was almost always required by terrestrial network operators with the well-established splice recipes and 1310 nm compatibility associated with that standard. However, the use of large A_{eff} fibers in terrestrial networks has recently become more important as a means to achieve longer reach lengths for high data rate systems with high-density modulation formats such as polarization multiplexed 16-quadrature amplitude modulation (PM-16QAM). To address this need, a new ITU-T G.654.E standard for terrestrial applications was approved in November 2016, with a specification for maximum mode field diameter (MFD) at 1550 nm to be 12.5 μm with ±0.7 μm allowable deviation[1]. This corresponds to a nominal effective area range of 125–130 μm^2, and an overall allowable range of A_{eff} of approximately 115–140 μm^2. In order to ensure that macrobend loss performance would be the same as for standard G.652 fibers (0.1 dB total loss for 100 turns with 60 mm diameter at 1625 nm), the cable cutoff wavelength specification for the new G.654.E fibers was increased from 1260 nm to 1530 nm.

Given this new terrestrial fiber standard, it is important to assess the expected transmission performance as measured against conventional G.652 fibers, as well as address other potential areas in which the G.654.E and G.652 fibers differ. A recent study evaluated various optical characteristics of G.654.E fiber samples from several sources in a field trial condition, but without providing detailed transmission performance data[2]. In this work we perform modeling and experiments to quantify the expected performance of a G.654.E-compliant fiber in EDFA-only systems, and in Raman-assisted systems with two different levels of available Raman pump power. For EDFA system modeling we use the analytical Gaussian noise model[3] to assess fiber figure of merit (FOM) in a relative sense and to quantify the absolute transmission performance. Experimental measurements are carried out with a re-circulating loop to compare PM-16QAM transmission performance of a G.654.E-compliant fiber to a G.652 fiber. We experimentally demonstrate at least 55% reach increase with a new G.654.E-compliant fiber compared to similar system configurations using a standard single-mode fiber. We also explore two areas potentially affected by the higher cable cutoff wavelength

Next-Generation Optical Communication: Components, Sub-Systems, and Systems VII, edited by Guifang Li, Xiang Zhou, Proc. of SPIE Vol. 10561, 105610N · © 2018 SPIE
CCC code: 0277-786X/18/$18 · doi: 10.1117/12.2297683

specification, namely the effect of Raman pump wavelengths propagating below the cable cutoff, and optical supervisory channels (OSCs) transmitted at wavelengths below the cable cutoff. We show that negligible impact is predicted or observed in either case, demonstrating that the longer cutoff wavelength will have no adverse effects for OSCs or Raman pumps.

The rest of the paper is organized in the following manner. In section 2, we describe the characteristics of a G.654.E fiber, model the relative FOM, and present modeling results of transmission in EDFA-only systems with different span lengths and two different 200 Gb/s modulation formats. In section 3, we present experimental re-circulating loop transmission results for both EDFA and hybrid Raman/EDFA systems with two different span lengths. In section 4, we explore potential impacts of the higher cable cutoff specification in terrestrial systems in terms of Raman pump propagation below cable cutoff, and OSC transmission at wavelengths well below cable cutoff. We find no expected measurable penalties in either case. Conclusions are drawn in section 5.

2. G.654.E FIBER DESIGN, CHARACTERISTICS, AND MODELING RESULTS

2.1 Fiber design

Corning® TXF™ fiber was designed to meet the new terrestrial G.654.E standard. Some of its key optical characteristics are shown in Table 1 along with those of a typical standard G.652 fiber. TXF is a silica-core fiber, with a fluorine-doped cladding to create a difference in refractive index between the core and the cladding. This type of fiber design is effective in producing lower overall attenuation compared to Germania-doped fibers (usually 0.18-0.20 dB/km). It also results in lower nonlinear refractive index, which along with the larger effective area improves the tolerance towards nonlinear effects. The larger effective area (compared to G.652 fibers) also necessitates an increase in TXF fiber dispersion, which happens to further improve nonlinear tolerance. The maximum cable cutoff wavelength for TXF fiber is set to 1520 nm (the G.654.E standard allows up to 1530 nm), and its macrobend loss performance meets the specifications defined to be the same in the G.652 and G.654.E standards. It is worth noting that the average splice loss of TXF fiber to itself is lower than the loss between like G.652 fibers, due to the larger MFD[4]. This is important given the large number of intra-span splices that are typical in terrestrial systems. On the other hand, the splice loss of TXF fiber to a G.652 fiber pigtail that might occur at amplifier sites is larger because of the MFD mis-match. However, such splices only occur twice in each span, and only the splice at the span end actually has an impact on span loss.

Table 1. Average fiber characteristics at 1550 nm.

	Standard G.652 fiber	**TXF fiber (G.654.E)**
Attenuation (dB/km)	0.189	0.168
Effective area (μm^2)	82	125
Estimated NL index n_2 (m^2/W)	$2.3x10^{-20}$	$2.2x10^{-20}$
Chromatic dispersion (ps/nm-km)	16.5	21
Peak Raman gain coefficient at 1450 nm (1/W/km)	0.4	0.25
Splice loss to self (dB)	0.03	0.02
Splice loss to G.652 fiber (dB)	0.03	0.15

2.2 Fiber figure of merit

To compare the expected performance of different optical fibers in modern coherent transmission systems with no in-line dispersion compensation, a figure of merit[5] (FOM) has been developed based on the Gaussian noise model. A simplified version of the FOM is used here as defined in Eq. 1. This FOM is defined such that it relates directly to the expected system Q-factor difference between the fiber under consideration and a reference fiber based on the relative attributes of the fibers.

$$\text{FOM(dB)} = \frac{2}{3}10\log\left[\frac{A_{eff}\cdot n_{2,ref}}{A_{eff,ref}\cdot n_2}\right] - \frac{2}{3}(\alpha_{dB}-\alpha_{dB,ref})\cdot L + \frac{1}{3}10\log\left[\frac{\alpha_{dB}}{\alpha_{dB,ref}}\right] + \frac{1}{3}10\log\left[\frac{D}{D_{ref}}\right] \quad (1)$$

In Eq. 1, α_{dB} and $\alpha_{dB,ref}$ are the attenuation values in dB/km for the fiber under consideration and the reference fiber, respectively. Similarly, D and D_{ref}, A_{eff} and $A_{eff,ref}$, n_2 and $n_{2,ref}$ are the respective dispersion, effective area, and nonlinear index values. L is the span length. The FOM for TXF fiber relative to a standard G.652 fiber as calculated from the fiber attributes in Table 1 is shown in Fig. 1a. In Fig. 1b, the FOM components of the different fiber characteristics of TXF fiber are shown for three representative span lengths. The results show that TXF fiber offers a FOM advantage over typical G.652 fiber of close to 3 dB for a system with 100 km span lengths and more than that for longer span lengths. Furthermore, the contributions to this FOM advantage from lower attenuation and larger A_{eff} are roughly equal, while the lower n_2 and higher dispersion values of TXF fiber also make smaller contributions.

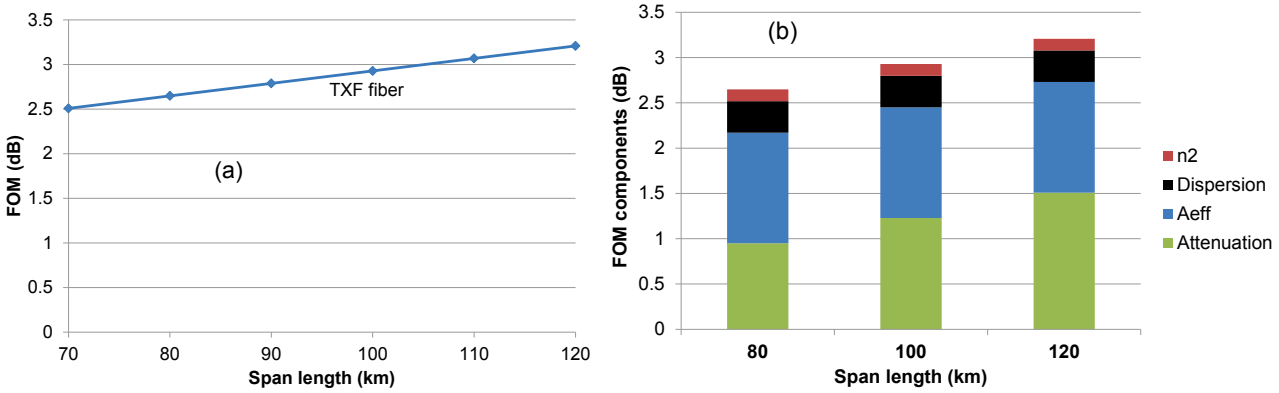

Figure 1: a) Fiber FOM relative to a typical standard G.652 fiber vs. span length, b) TXF fiber FOM components for three span lengths.

2.3 Transmission modeling of PM-16QAM and PM-8QAM systems with EDFA-only amplification

To gain an understanding of the absolute reach lengths potentially possible with TXF fiber and standard single-mode fiber, we first modeled the transmission performance at the distances of 1500 km and 3000 km for 200 Gb/s channels with EDFA-only amplification[6]. Two 200 Gb/s signal types were studied: 33 Gbaud PM-16QAM and 44 Gbaud PM-8QAM. We assumed a 5.5 dB soft decision forward error correction (SD-FEC) threshold, 5 dB EDFA noise figure, 96 WDM channels, 5 km cable drum length (which determines the number of splices per span), the splice losses given in Table 1, and 0.5 dB of total connector loss per span split between the two ends. We also included a relative implementation penalty for both formats of about 2.7 dB at 1x10-3 BER to represent realistic transponder equipment performance. The modeling was performed using the framework of the Gaussian noise model for coherent systems[3]. For the standard G.652 fiber, we used Corning SMF-28e+® fiber, which has the same general characteristics as shown in Table 1.

Fig. 2a shows that for a 1500 km link, both fiber types have Q values that exceed the 5.5 dB FEC threshold for almost all span lengths. On the other hand, if at least 3 dB Q margin is required (as is usual), then the PM-8QAM format must be used with SMF-28e+ fiber, while the PM-16QAM format can still be employed with TXF fiber (thus allowing higher spectral efficiency) up to 100 km span lengths. For a 3000 km link (Fig. 2b), the SMF-28e+ fiber systems with either format are unable to demonstrate 3 dB Q margin. However, 200 Gb/s signals generated with the 44 Gbaud PM-8QAM format and transmitted over TXF fiber exceed the 8.5 dB Q threshold for span lengths at least up to 90 km. Therefore the TXF fiber may allow 3000 km reach lengths with sufficient Q margin using the 8QAM format and relatively long span lengths.

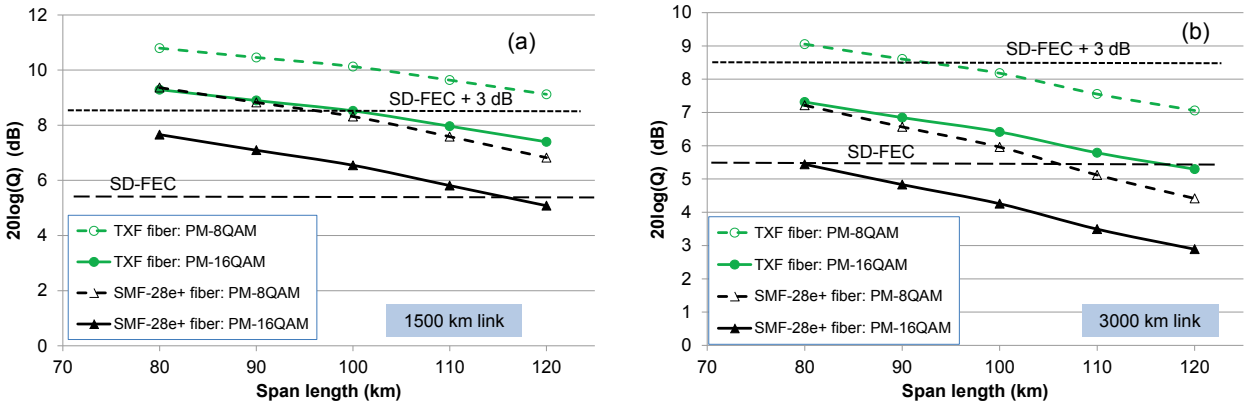

Figure 2: a) Q-factor vs. span length for 200 Gb/s PM-16QAM and PM-8QAM systems at a) 1500 km and b) 3000 km.

3. RE-CIRCULATING LOOP TRANSMISSION EXPERIMENTS WITH PM-16QAM

We next conducted transmission experiments of 256 Gb/s PM-16QAM signals over 75 km and 100 km spans of TXF fiber and SMF-28e+ fiber in a re-circulating loop with 20 DWDM channels. We chose to concentrate only on 16QAM transmission performance, and the baud rate was 32 Gbaud. The general loop set-up was previously described[7] and is illustrated in Fig. 3. The implementation penalty at $1x10^{-3}$ BER for our laboratory transmitter and receiver was relatively large at about 3.6 dB, at least partially due to bandwidth limitations in the transmitter. Two system configurations were investigated: 1) EDFA-only amplification, and 2) Raman-assisted, or hybrid Raman/EDFA amplification with 500 mW or 1000 mW of total Raman pump power. The Raman pumping configuration was counter-propagating to the signal, and the average Raman ON/OFF gain values measured for 100 km spans with 500 mW total pump power was about 9.2 dB for TXF fiber and 15.4 dB for SMF-28e+ fiber. For 1000 mW pump power, the Raman gain measured in 100 km of TXF fiber was about 14.5 dB. The higher pump power was not used with SMF-28e+ fiber as it was not expected to provide significant benefit.

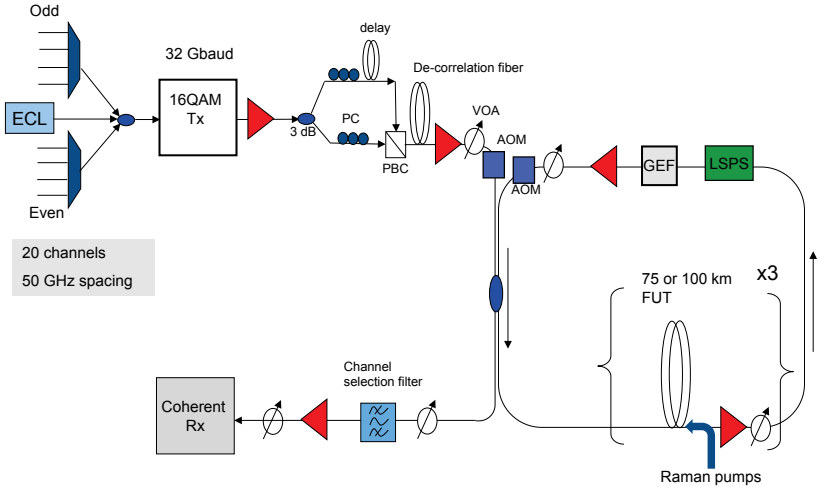

Figure 3: Schematic illustration of re-circulating loop transmission systems configuration.

The 100 km span transmission results for a central channel at 1550.92 nm are given in Fig. 4a, with Q-factor values calculated from BER measurements given as a function of distance for EDFA-only and hybrid Raman/EDFA transmission systems. The 5.5 dBQ FEC threshold and 8.5 dBQ levels (3 dBQ margin) are also shown in Fig. 4a. The data in the figure show several things. One is that for EDFA-only systems, TXF fiber provided ~55% longer reach length than SMF-28e+ fiber. Another is that the TXF fiber EDFA-only system produced essentially the same performance and reach lengths as the hybrid Raman/EDFA system with SMF-28e+ fiber, thus providing comparable performance with lower cost amplification units. The greatest reach was found with TXF fiber with hybrid

Raman/EDFA amplification with 1000 mW Raman pump power, which was able to achieve over 2000 km reach length (with 3 dBQ margin) for 100 km spans. Similar data for both fibers and amplification schemes for 75 km spans are shown in Fig. 4b. In this case, we find that the hybrid Raman/EDFA system with TXF fiber and 500 mW pump power can also achieve over 2000 km reach. For the EDFA-only systems, the TXF fiber again offers ~53% reach advantage over the system with SMF-28e+ fiber. The reach length data for all systems with 3 dBQ margin is summarized in Fig. 5. The results show that TXF fiber has a reach length longer than 1500 km with 3 dBQ margin in 4 out of 5 systems tested, and longer than 2000 km with hybrid Raman/EDFA amplification in two system configurations. The reach advantage demonstrated with TXF fiber over the standard single-mode fiber was up to 55%. We note that longer absolute reaches than these will be possible in straight-line systems without loop effects, with smaller transceiver implementation penalties likely with commercial equipment, and with EDFAs optimized to work in combination with Raman amplifiers in a hybrid design.

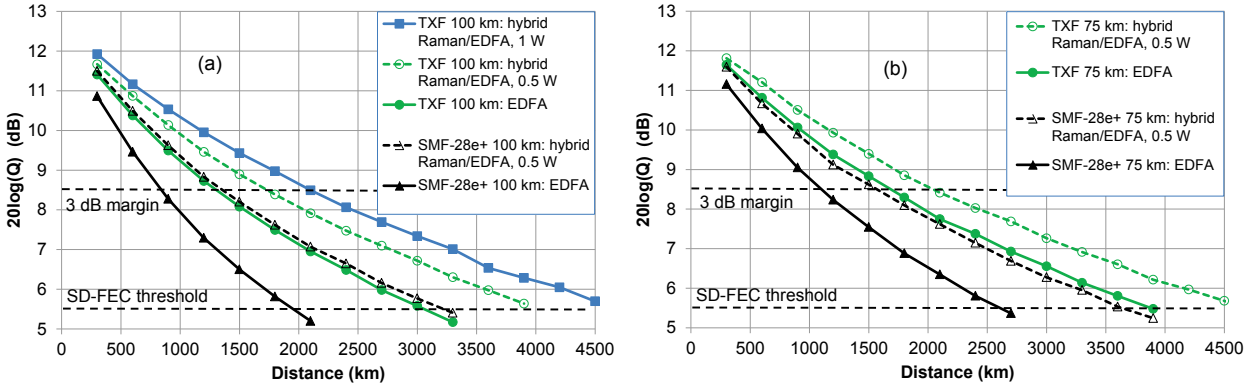

Figure 4: Re-circulating loop transmission results for a) 100 km spans, and b) 75 km spans.

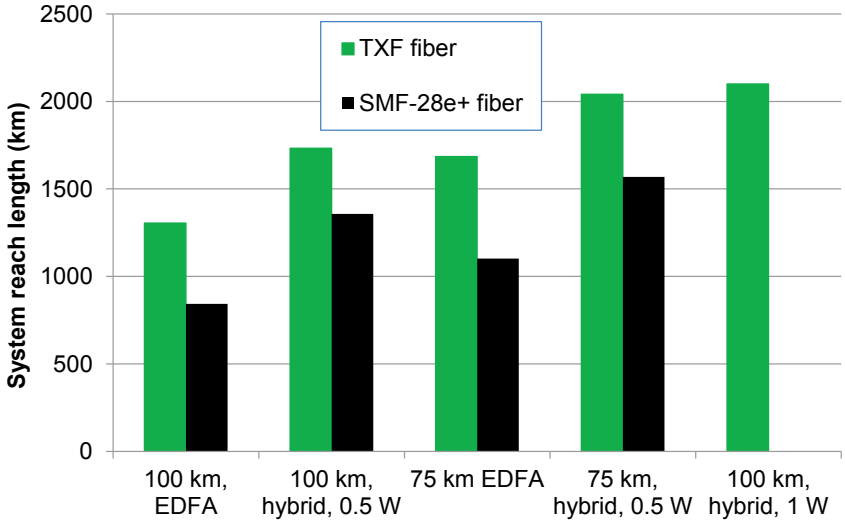

Figure 5: Summary of system reach lengths at 8.5 dBQ (3 dB margin over SD-FEC threshold) for different system configurations.

4. IMPLICATIONS OF LONGER CABLE CUTOFF IN TERRESTRIAL SYSTEMS

4.1 Analysis of Raman pump propagation below cable cutoff

Given that the maximum cable cutoff wavelength specification for G.654.E fibers is defined as 1530 nm, and the fact that hybrid Raman/EDFA amplification is becoming more widely used in terrestrial systems, it is worthwhile to consider if there may be possible effects on received signal quality from Raman pump propagation below the cable cutoff[8]. In particular, the question becomes whether multi-path interference (MPI) occurring in Raman pump wavelengths can

affect signal quality in the transmission band through transfer of pump relative intensity noise (RIN) to signal RIN and phase noise. The effects of Raman pump RIN on signal quality have been studied previously[9,10]. Here, we address the magnitude and effects of pump RIN specifically induced by MPI that is a function of distance into a span due to non-single-mode propagation. We will find the effect to be very small or negligible even under several worst-case conditions likely to be unrepresentative of normal systems.

The model employed to analyze MPI growth in a lightwave propagating below cable cutoff in a given span was described earlier[11,12]. In this model, we assume that coupling between the fundamental mode LP_{01} and the higher order mode assumed to be LP_{11} occurs at the splice points within the span, and potentially also via continuous distributed coupling along the fiber through microbending effects. At the splice points, we assume that for a Raman pump with wavelength below cable cutoff, any splice loss $L_{splice}[dB]$ effectively results in the lost optical power being coupled from LP_{01} to LP_{11} with power coupling coefficient given by $\varepsilon = 1 - 10^{-L_{splice}[dB]/10}$. By reciprocity, optical power propagating in LP_{11} will couple back to LP_{01} with the same coefficient and in this way MPI is generated through multiple crosstalk terms with different delays relative to the main pump transmission. MPI is defined as the ratio of total crosstalk power to average un-coupled pump power in the LP_{01} mode as

$$MPI = \frac{P_{xtalk,total}}{P_{pump,ave}} = \frac{\sum_1^N P_{xtalk,n}}{P_{pump,ave}} \quad . \tag{2}$$

If distributed mode coupling is also present, the total crosstalk power will include this contribution in addition to the splice-generated terms[12,13].

To model the MPI generation, we assume a link with the following characteristics: span length L_{span} = 100 km, intra-span splice interval = 4 km, Raman pump LP_{01} attenuation at 1450 nm α_P of 0.21 dB/km, and differential mode attenuation (DMA) of the pump laser between LP_{01} and LP_{11} is 0.0 dB/km (worst-case). For a large effective area G.654.E transmission fiber, we assume a conservative 0.2 dB splice loss at the beginning and end of each span to standard G.652 fiber at amplifier sites. Results from the MPI generation model are shown in Fig. 6a, demonstrating MPI growth in the Raman pump as a function of distance into the span for three different intra-span average splice loss levels. To model the worst-case condition under which pump RIN would have the greatest effect on signal quality, we assume that the Raman pump is launched in the same direction as the transmission signals here from the beginning of the span (co-pumping). Another worst-case condition in which the splices are configured in a straight-through state without ~80 mm diameter fiber loops on each side of the splice is also incorporated into the model. If present, as is usual in terrestrial splice trays, such fiber loops would preferentially attenuate the LP_{11} mode and substantially reduce MPI growth[12].

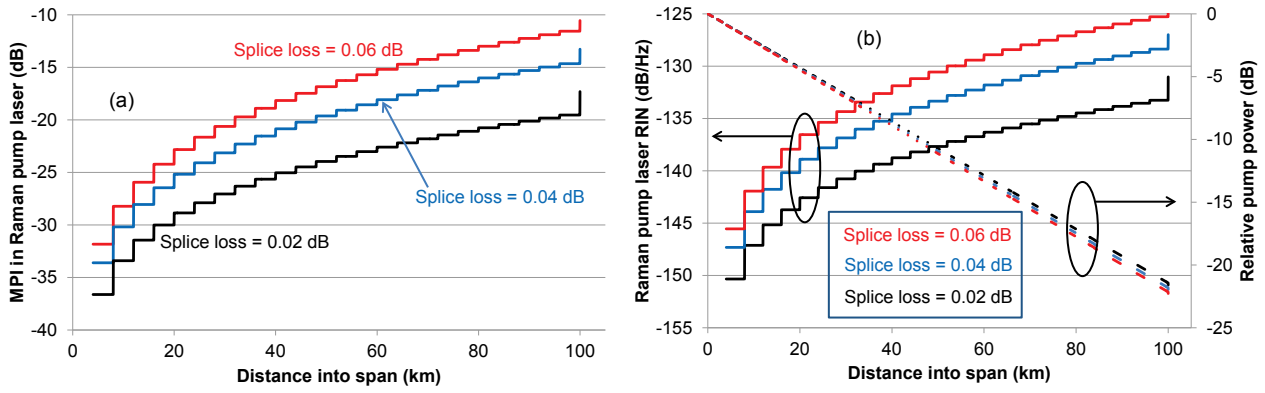

Figure 6: a) MPI growth as function of distance into span for different splice losses, b) Raman pump RIN and relative pump power level as function of distance into span.

The relationship between pump laser MPI and pump laser RIN is given for incoherent crosstalk terms by[14]

$$RIN_P(f) \approx \frac{4 \cdot MPI}{\pi}\left[\frac{\Delta\nu}{f^2 + (\Delta\nu)^2}\right] \tag{3}$$

where f is frequency and $\Delta\nu$ is the pump laser linewidth (~300 GHz). Thus the pump RIN will increase as a function of distance into the span proportional to the pump MPI. Fig. 6b illustrates this dependence along with the relative pump power evolution in the span. We see that the MPI-induced pump RIN is smallest where the pump power is largest since the MPI grows with distance while power decreases.

To incorporate the effect of pump laser MPI into the performance evaluation of signal quality in a transmission system with Raman amplification, we adopt the framework employed in Ref. [9], and extend it to capture the effect of *z*-dependent MPI and pump RIN, RIN_P. We assume co-propagating Raman amplification with an undepleted pump approximation, since signal noise generated by counter-propagating RIN_P is much smaller[9], and we focus our analysis on a worst-case scenario evaluation. The details of the analysis were given earlier[8]. Here we present the basic results for the effects of MPI-induced pump RIN on signal quality in terms of signal RIN and the more dominant effect of signal relative phase noise. To illustrate the effects, we modeled a fiber with Raman gain coefficient representative of a large A_{eff} fiber, and Raman pump power sufficient to effect On-Off gain = 19 dB to compensate for total signal loss from fibre, splices, connectors, etc.. The attenuation at the nominal pump wavelength of 1450 nm is 0.21 dB/km, and we modeled systems with 100 km span lengths.

As mentioned above, the dominant impairment for coherent systems is signal relative phase noise. The penalty in terms of signal-to-noise ratio (SNR) per bit at a BER value of $1x10^{-3}$ as a function of the total phase error variance arising from all sources is shown in Fig. 7 for four different modulation format signals. To isolate the impairment penalty arising from MPI-induced pump RIN impressed on the signal, we look specifically at the two formats of PM-16QAM and PM-16PSK in Fig. 8. The system modeled was a 3000 km link with 32 Gbaud polarization multiplexed 256 Gb/s channels. We assumed a distributed coupling coefficient value of $k = 10^{-4}$ km^{-1}. This data shows that the penalty expected is extremely small so as to be negligible even for splice loss values up to 0.07 dB. Thus we find that the signal SNR per bit penalty induced by Raman pump MPI due to propagation below cable cutoff in G.654.E fibers is insignificant in long haul system links. This is true even for unrealistic worst-case conditions of co-propagating Raman pumps, higher than expected splice losses, 0 dB/km differential mode attenuation in the fiber, and no fiber loops in splice trays that would preferentially attenuate the LP_{11} mode. This should allay concerns as to any impairments arising from Raman pump propagation below cable cutoff in terrestrial systems.

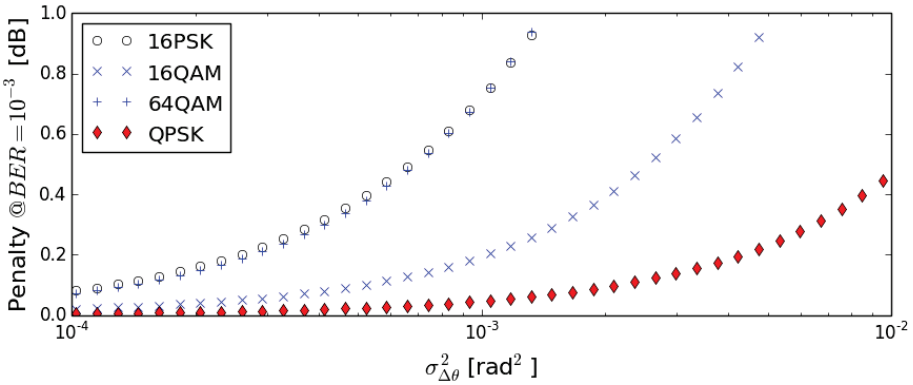

Figure 7: SNR per bit penalty at a BER value of $1x10^{-3}$ as a function of total phase error variance for four different polarization multiplexed modulation formats.

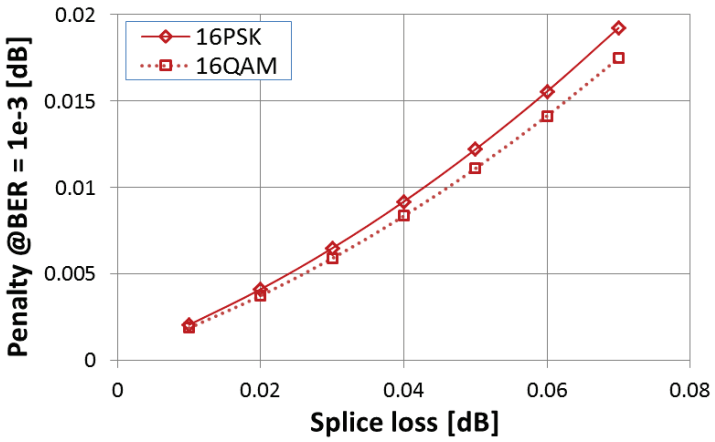

Figure 8: SNR per bit penalty at a BER value of $1x10^{-3}$ generated from MPI-induced Raman pump RIN as a function of intra-span splice loss.

4.2 Optical supervisory channel transmission below cable cutoff

Another potential concern in terrestrial systems that may arise regarding G.654 fibers with cable cutoff values up to 1520 nm or 1530 nm is optical supervisory channel (OSC) transmission below cable cutoff[11]. The OSC is a low data-rate (<2.5 Gb/s) optical channel located outside of the main transmission band that communicates system and control information between optical amplifier sites. In particular, the wavelength of 1510 nm is often used for OSC transmission[15]. Since 1510 nm falls below the cable cutoff wavelength specification of the new G.654.E fiber standard, there is the potential that OSC transmission performance could be adversely impacted by multi-path interference (MPI). In this section we address the issue of low data rate transmission representing an OSC at wavelengths below the cable cut-off. While higher order modes (typically LP_{11}) may be excited below cable cutoff, the level of MPI generated depends on the coupling between LP_{01} and LP_{11} at splice points, as shown earlier, and the DMA between LP_{01} and LP_{11} in the cabled fiber and bend loss induced in splice trays. We have investigated a cabled span of G.654.B fiber for reasons of availability through extensive MPI and OSC transmission measurements. In a worst-case configuration without splice tray loops, we demonstrate no power penalty up to 40 nm below cut-off, and the MPI measurements suggest there may be no penalty even 60-80 nm below cable cutoff.

The model of the expected MPI growth in a span supporting two modes was described in the previous section as arising primarily at the intra-span splice points, as well as from continuous distributed mode coupling within the fiber. It is also strongly dependent on the DMA as was shown previously[11,13]. To understand the OSC penalty that might arise from MPI, we first made experimental measurements using a controlled MPI emulator[16] with 8 individual crosstalk terms for a 2.5 Gb/s NRZ signal. The extinction ratio of the signal was 10 dB. The crosstalk terms were randomly polarized and delayed with respect to each other and the signal, as will likely be in the case for splice-generated MPI. The results in Fig. 9 show that MPI values < -32 dB produce negligible penalty.

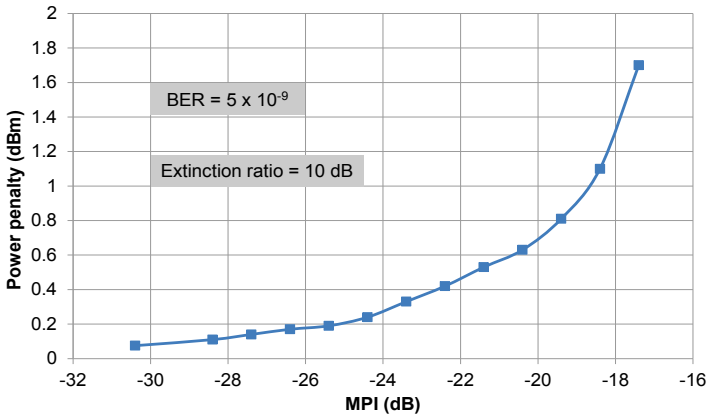

Figure 9: Measured power penalty from MPI with randomly polarized crosstalk terms for a 2.5 Gb/s NRZ signal.

To conduct MPI characterization and transmission experiments, we cabled an ITU-T G.654.B compliant fiber (Corning® Vascade® EX2000 optical fiber) in two gel-filled buffer tubes, each of length 4.2 km. Note that the maximum cable cutoff specification for ITU-T G.654.B is the same as for ITU-T G.654.E, and this fiber type was used in the experiments due to availability with the expectation that the behavior would be representative due to the similar cutoff. Each tube contained 11 Vascade EX2000 fibers (along with 1 other un-used fiber), which formed a 92.4 km span with a total of 21 intra-span splices when spliced together. The G.654 fiber was spliced to standard single-mode fiber jumpers at the input and output ends of the span. The fiber deployed in the tubes was taken from two source reels, with cable cutoff wavelengths of 1520 nm and 1480 nm. The cabled fiber span is illustrated schematically in Fig. 10.

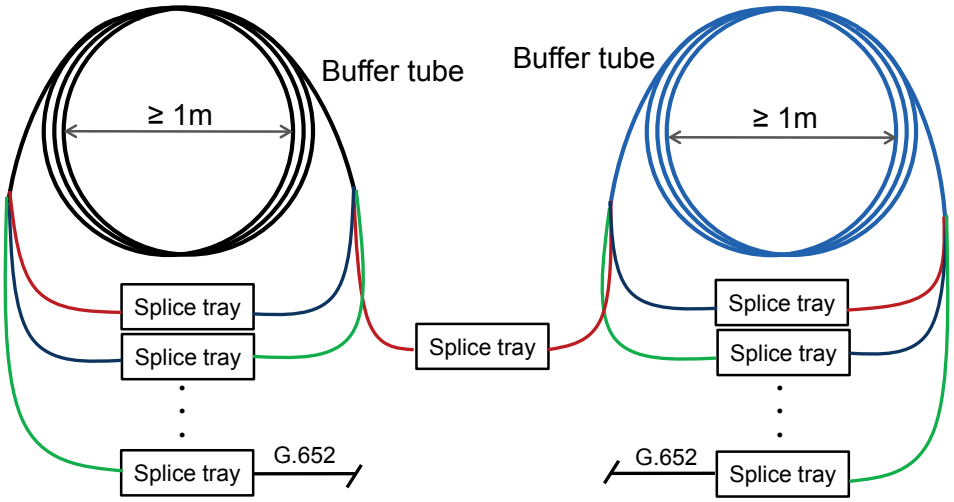

Figure 10: Experimental configuration with 92.4 km cabled span of G.654 fiber.

To create a worst-case condition again, we spliced the fibers together without introducing the usual several ~80 mm diameter loops on each side of the splice as done in terrestrial splice trays. Each splice section was kept straight, creating a condition for maximum MPI generation. We measured MPI generated by propagation through the span as a function of wavelength by analysis of the power fluctuations of a CW laser transmitted through the span[16]. The measurement results are shown in Fig. 11. Even at wavelengths as low as 1420 nm, the MPI is ≤ -35 dB. According to the data in Fig. 9, these MPI results predict negligible OSC penalty over the whole wavelength range measured. We note that 1420 nm is about 60 nm below cutoff of the fiber comprising half the span, and 100 nm below cut-off of the rest of the fiber. Also shown in Fig. 11 is the range of back-to-back MPI measurements, illustrating an effective measurement floor.

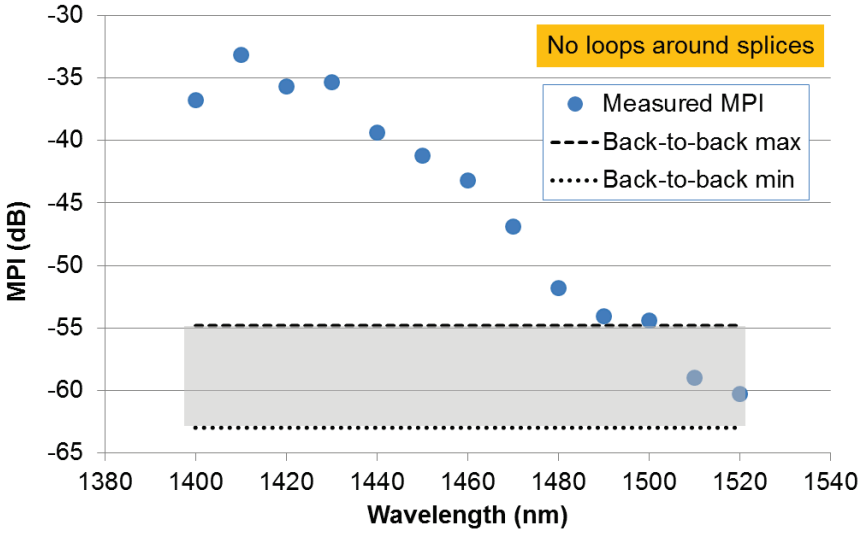

Figure 11: Experimentally measured MPI data through 92.4 km cabled span of G.654 fiber.

The results in Figs. 9 and 11 suggest that negligible penalty should be observed for transmission through the 92.4 km span even for wavelengths down to 1440 nm and possibly lower. We tested this by transmitting a 2.5 Gb/s NRZ signal with 10 dB extinction ratio over the fiber span. A tunable laser and external Mach-Zehnder modulator (MZM) allowed various wavelengths to be studied. The received power was controlled with a variable optical attenuator (VOA) and the receiver was a 2.5 Gb/s laboratory unit with clock and data recovery. We made transmission measurements of bit error rate (BER) as a function of received power in back-to-back (B2B) and through the 92.4 km cabled fiber span for several wavelengths. Fig. 12 shows results for transmission at 1440 nm and 1480 nm. We observe essentially no penalty for transmission through the span compared to back-to-back, even though 1440 nm is 40 nm below the cut-off of the lowest cut-off fibre in the tubes. This confirms the expectation of insignificant penalty given the small MPI measurements. Similar measurements at 1460 nm for an OSC signal with 6.0 dB extinction ratio (more susceptible to MPI impairments) also showed no penalty.

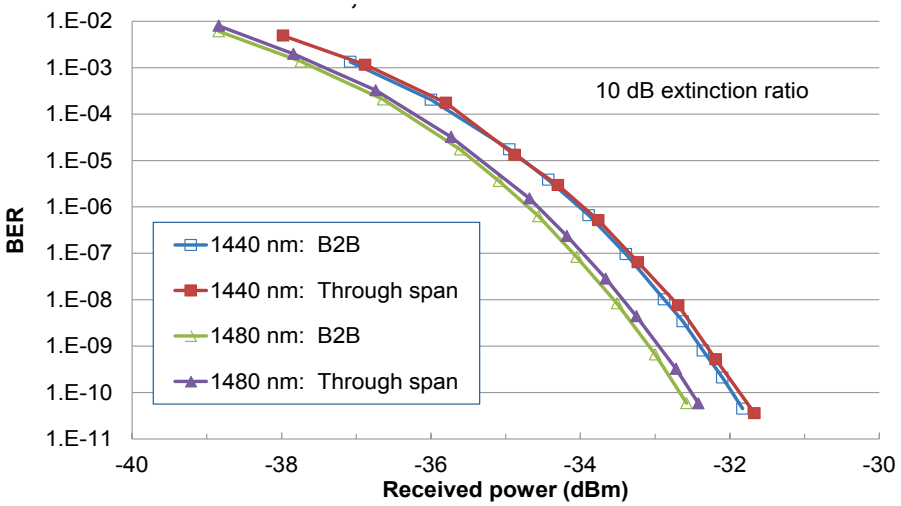

Figure 12: BER vs. received power for a 2.5 Gb/s OSC through the cabled fiber span and back-to-back at 1440 nm and 1480 nm. .

5. CONCLUSIONS

We have discussed the introduction of a new fiber standard G.654.E for terrestrial transmission systems. We presented modeling and experimental transmission results of Corning TXF fiber that was designed to meet the requirements of the new standard. We demonstrated significant experimentally measured reach advantages of up to 55% of TXF fiber in comparison to standard G.652 single-mode fiber for 256 Gb/s PM-16QAM signals in re-circulating loop experiments with both EDFA-only and hybrid Raman/EDFA amplification schemes and two span lengths of 75 km and 100 km. The TXF fiber systems achieved reach lengths with at least 3 dBQ margin greater than 1500 km in four system configurations, and greater than 2000 km in two configurations. We then examined two areas that could potentially be affected by the longer cable cutoff wavelength of the G.654.E standard, namely Raman pump propagation below cable cutoff, and optical supervisory channel transmission below cable cutoff. We determined through modeling, analysis, and experimental measurement that negligible penalties are expected for either effect, even with worst-case conditions not found in realistic systems. Thus G.654.E fiber such as TXF fiber offers significant reach and performance advantages for high data rate signals in long haul terrestrial systems.

ACKNOWLEDGEMENTS

The authors would like to thank Aramais Zakharian, Nikolay Kaliteevskiy, Sergey Ten, Steven Garner, Jeremy Blaker, Stephen Wright, Chris Towery, Greg Mills, and Maurice O'Sullivan for significant contributions to this work.

REFERENCES

[1] Recommendation ITU-T G.654 (2016), Characteristics of a cut-off shifted single-mode optical fibre and cable.

[2] Shen, S., Wang, G., Wang, H., He, Y., Wang, S., Zhang, C., Zhao, C., Li, J., and Chen, H. "G.654.E Fiber Deployment in Terrestrial Transport System," OFC 2017, paper M3G.4 (2017).

[3] Poggiolini, P., "The GN Model of Non-Linear Propagation in Uncompensated Coherent Optical Systems," J. Lightwave Technol. **30**, 3857-3879 (2012).

[4] Makovejs, S., Downie, J. D., Hurley, J. E., Clark, J. S., Roudas, I., Roberts, C. C. Matthews, H. B., Palacios, F., Lewis, D. A., Smith, D. T., Diehl, P. G., Johnson, J. J., Towery, C. R. And Ten, S. Y., "Towards superior transmission performance in submarine systems: leveraging ultra-low attenuation and large effective area," J. Lightwave Technol. **34**, 114-120 (2016).

[5] Curri, V., Carena, A., Bosco, G., Poggiolini, P., Hirano, M., Yamamoto, Y., and Forghieri, F., "Fiber figure of merit based on maximum reach," OFC 2013, paper OTh3G.2 (2013).

[6] Downie, J. D., Makovejs, S., Kaliteevskiy, N., Hurley, J., Wright, S., and Towery, C., "Transmission Performance of Large A_{eff} Ultra-Low-Loss Terrestrial Fibre in 200 Gb/s EDFA and Raman-Assisted Systems," ECOC 2017, paper P1.SC1.6 (2017).

[7] Downie, J. D., Hurley, J., Pikula, D., Ten, S., and Towery, C., "Study of EDFA and Raman system transmission reach with 256 Gb/s PM-16QAM signals over three optical fibers with 100 km spans," Opt. Express 21, 17372-17378 (2013).

[8] Mlejnek, M., Downie, J. D., and O'Sullivan, M., "Analysis of Potential Terrestrial System Effects from Raman Pumps below Cable Cut-off in G.654.E Fibres," ECOC 2017, paper P1.SC1.14 (2017).

[9] Cheng, J., Tang, M., Fu, S., Shum, P., Yu, D., and Liu, D., "Relative phase noise induced impairment in M-ary phaseshift-keying coherent optical communication system using distributed fiber Raman amplifier," Opt. Lett., 38, 1055-1057 (2013).

[10] Cheng, J., Tang, M., Fu, S., Shum, P., Yu, D., Wang, L., and Liu, D., "Relative Phase Noise-Induced Phase Error and System Impairment in Pump Depletion/Nondepletion Regime," J. Lightwave Technol., 32, 2277-2286 (2014).

[11] Downie, J. D., Hurley, J., DePedro, H., Garner, S., Blaker, J., Zakharian, A., Ten, S., and Mills, G., "Investigation of Potential MPI Effects on Supervisory Channel Transmission below Cable Cut-off in G.654 Fibres," ECOC 2016, paper Th.2.P2.SC5.50 (2016).

[12] Downie, J. D., Hurley, J., DePedro, H., Garner, S., Blaker, J., Zakharian, A., Ten, S., and Mills, G., "Measurements and modeling of multipath interference at wavelengths below cable cut-off in a G.654 optical fiber span," Opt. Express, 25, 9305-9311 (2017).

[13] Mlejnek, M., Roudas, I., Downie, J. D., Kaliteevsky, N., and Koreshkov, K., "Coupled mode theory of multipath interference in quasi-single mode fibers," IEEE Photonics Journal, **7**(1), 1-16 (2015).

[14] Gimlett, J. L. and Cheung, N. K., "Effects of Phase-to-Intensity Noise Conversion by Multiple Reflections on Gigabit-per-Second DFB Laser Transmission Systems," J. Lightwave Technol. 7, 888-895 (1989).

[15] Sarkar, C., "Optical Supervisory Channel Implementation," Int. J. Sci. Eng. Res. 3, 1-3 (2012).

[16] Downie, J. D., Hurley, J., Roudas, I., Koreshkov, K., and Mlejnek, M., "MPI Measurements of Quasi-Single-Mode Fibers," IEEE Phot. Conf. (IPC), paper MG3.4 (2015).